


An adaptive scheduling scheme for inhomogeneously distributed wireless ad hoc networks

Adnan FAZIL^{1,*}, Aamir HASAN², Muhammad Atique Ur REHMAN¹,
Ijaz Mansoor QURESHI¹

¹Air University, Islamabad, Pakistan

²Dhanani School of Science & Engineering, Habib University, Karachi, Pakistan

Received: 03.11.2018

Accepted/Published Online: 08.04.2019

Final Version: 26.07.2019

Abstract: An efficient scheduling strategy guarantees the simultaneous transmission and successful reception by the scheduled nodes even inside a congested wireless ad hoc network. Owing to the dispersed nature of ad hoc networks, the node packing algorithm needs to be implementable without having network-wide channel state information and should additionally be able to pack the optimum number of successful transmissions. The proposed algorithm, for a network with nonhomogeneously distributed nodes, makes the decision to either inhibit or permit an active interferer around an active receiver based on the interferer's transmission power. The analysis evidenced that the suggested scheme provides an estimated 100 times superior transmission capacity when equated to the random aloha scheme. Moreover, the proposed strategy proved its vitality by demonstrating substantial improvement in transmission and transport capacity in comparison to the preexisting renowned scheduling schemes for distributed networks. The final results present a closed-form formula for the best possible exclusion-zone size multiplier factor in terms of the network parameters, i.e. the network's path-loss exponent, spreading gain, SINR threshold, outage constraint, and Tx-Rx separation.

Key words: Node scheduling, MAC protocol, exclusion zone, ad hoc networks, transmission capacity

1. Introduction

The topology of wireless ad hoc networks holds great potential for emerging technologies, such as mesh networks, machine-to-machine (M2M) communication, and the Internet of things (IoT). Moreover, the research community is pursuing dense wireless networks of shorter communication links between different communication devices [1, 2], owing to the IoT's plethora of potential applications. Consequently, M2M communication technology is improving to enhance the energy efficiency, spatial reuse, and spectral efficiency by utilizing smaller transmitter-receiver (Tx-Rx) separations with a large number of devices [3, 4]. On top of that, the model of the medium access control (MAC) protocol for these distributed networks is a critical factor for their transmission handling ability owing to the arbitrarily dispersed transceivers with coincident transmissions in the spatial proximity as well as at the same frequency [5–7]. The nature of M2M communication requires the MAC protocol to be enforced in an uncomplicated yet effective way that is actually resilient against outages due to nearby interferers. Hence, ad hoc networks have been the leading area of investigation for the last few years [5, 8–10].

The research community has also valued the benefits garnered by spread spectrum-based MAC using code division multiple access (CDMA) for wireless ad hoc networks, due to its capability to significantly suppress

*Correspondence: adnan.fazil@mail.au.edu.pk

the interference levels and enhance the spatial reuse [5, 11–14]. Nevertheless, the use of CDMA alone is deemed unjustifiable due to wastage of the precious RF spectrum for capacity improvement; therefore, alternate options have also been considered in combination with CDMA [5, 15, 16].

Different stochastic models have always been the mainstay of the simulation and analysis of distributed wireless ad hoc networks. However, most researchers employed distributions where nodes are randomly distributed in a homogeneous manner, either by applying the Poisson point process (PPP) or sampling from a uniform distribution, depending on the network characteristics. In contrast, the wireless transceivers in real-world scenarios are often nonhomogeneously distributed owing to the fact that at a given time the users are concentrated at different places such as specified pathways, markets, buildings, or playing fields. Surprisingly, this modeling anomaly exists even after disclosure of the crucial relationship between the nodes' distribution and the network transmission capacity [14, 17–19].

In this paper, we have investigated a new technique to implement an adaptive exclusion zone in an ad hoc network with nonhomogeneously distributed nodes. We have shown that the proposed adaptive scheduling scheme performs better than the random aloha scheme, the widely used carrier sense multiple access (CSMA) [20] scheme, and the system-wide fixed receiver guard zone scheme [5] in terms of the transmission capacity.

1.1. Related work and misconceptions regarding the nearest neighbor

Any wireless network requires an efficient channel access scheme to ensure the coexistence of different communication links in close spatial proximity [21, 22]. Under similar circumstances, different scheduling strategies are bound to perform variously with respect to different performance indicators, such as transmission capacity, the probability of outage, transmission delays, QoS, or energy consumption. In this paper, our principal objective is to optimize the scheduling algorithm to maximize the transmission capacity while neglecting the other effects.

In [23], a random design was applied to finally optimize the channel access scheme for an ad hoc network and a distributed MAC protocol was suggested in order to maximize spatial reuse through randomly sized exclusion zones around the nodes. The significant defect of the strategy ended up being its high likelihood ($> 50\%$) of failed transmissions and, consequently, poor resource utilization. The authors of [24] employed the multistage contention protocol in a distributed way and accomplished some promising results; nonetheless, they assumed a fixed separation between all the Tx-Rx pairs without any power control scheme. On the other hand, [25] proposed a CDMA-based MAC for an ad hoc network, but without overall performance evaluation in terms of spatial reuse. In addition, their work does not analyze the proposed protocol's ability to preserve the already developed links while accommodating new nodes in an established network.

The renowned IEEE 802.11 standard's MAC protocol for wireless networks [20] utilizes the CSMA scheme to schedule concurrent transmissions. The protocol uses virtual exclusion zones around each active transmitter to inhibit any interferer from transmitting within that zone. Thus, instead of safeguarding the receiver to enhance the chances of meeting the required SINR, the interferer is inhibited by another transmitter. However, a better approach is to incorporate exclusion zones around each active receiver to inhibit nearby interferers, as shown in [16], where an optimally sized guard zone was derived for a system with fixed transmission ranges. In [5], the authors used a system model with variable Tx-Rx separations, but they also proposed a fixed-sized exclusion zone around each active receiver.

The seminal research work in [26] explored many new research directions for the community. One of the major concepts was the exclusion zone or a guard zone around the receiver, which was contemplated by many researchers to significantly raise the wireless network's capacity [5, 15, 16, 20]. The network-wide fixed

receiver guard zone proved its strength in comparison to various other popular scheduling strategies in terms of transmission and transport capacity [5, 16]. However, all of these works were focused on inhibiting the closest interferer and the nearest neighbor distance is still believed to be a crucial parameter for a wireless network’s modeling and analysis [27, 28].

The closest interferer has always been considered the strongest and consequently the most deteriorating interferer. However, this is not the case unless the interferers’ transmitted power is constant. In contrast, under the proposed pairwise power control (explained later), an interferer’s transmission power is proportional to its own Tx-Rx separation and the nearest interferer is not bound to be the dominant one. For instance, we have two interferers, i.e. Tx₁ and Tx₂, placed at the same distance from an active receiver (Rx_o), where interferer Tx₁ is transmitting $P_1 = \rho(d_1)^\alpha$ to its receiver (Rx₁) placed at distance d_1 while interferer Tx₂ is transmitting $P_2 = \rho(d_2)^\alpha$ to its receiver (Rx₂) placed at distance d_2 , as shown in Figure 1. Now, if $d_2 = 3 \times d_1$ then

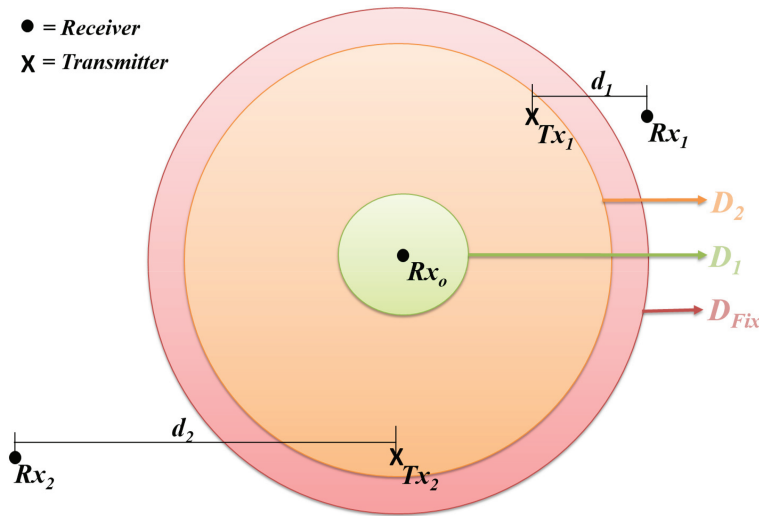


Figure 1. An example to show that the closest interferer is not always the strongest interferer and therefore the network-wide fixed guard zone size (D_{Fix}) is not the best choice for interference suppression while maximizing the transmission capacity.

$P_2 = 81 \times P_1$ for $\alpha = 4$ under PPC. Here, Tx₁ and Tx₂ are placed at the same distance from the subject receiver; however, Tx₁ is far less probable to cause an outage at the subject receiver as compared to the second interferer owing to its low transmission power.

Therefore, the probability that an interferer will cause an outage at a receiver is not solely dependent upon its distance from the receiver, but also directly proportional to the interferer’s Tx-Rx separation, under pairwise power control. Intuitively, it is thus extremely unfair to inhibit both the interferers with a large (fixed-sized) exclusion zone (D_{Fix}). Instead, an adaptive exclusion zone of radius $D = \Omega d_t$ should be incorporated to inhibit the interferer with Tx-Rx separation of d_t , where Ω is the network-wide fixed exclusion zone size multiplier or simply the exclusion zone multiplier and needs to be optimized for capacity maximization. Consequently, the interferer Tx₁ should be inhibited if it falls within the corresponding guard region (i.e. D_1), and similarly the interferer Tx₂ should be inhibited if it falls within the corresponding guard region (i.e. D_2), as shown in Figure 1.

1.2. Contributions

Most of the literature has focused on a network model with homogeneously distributed nodes according to a homogeneous Poisson point process (HPPP). Recently, nonhomogeneous and clustered networks have also been studied by different researchers [14, 27, 28]; however, an efficient scheduling scheme with a detailed comparison with the well-known existing schemes has not yet been proposed for these networks. Nevertheless, keeping in view the real-world scenario, we apply a technique to generate nonhomogeneous distribution and then highlight the need for adaptive exclusion zone-based scheduling by proposing and analyzing a variably sized exclusion zone scheme, which inhibits an interfering transmitter depending on the interferer's Tx-Rx separation. Here, we have explored the effect of an adaptive exclusion zone on the spatial reuse of the network, unlike the former schemes, which ensure spatial separation among the concurrent transmission by enforcing a fixed-sized exclusion zone around each active receiver where all the transmissions are inhibited except transmission by its intended transmitter. As the proposed exclusion zone's radius is a multiple of the interferer's Tx-Rx separation, we have derived a network-wide optimal multiplier, i.e. Ω^* , where each active receiver is surrounded by an exclusion zone of radius Ω^* times d_{ii} to inhibit the i th interferer, where d_{ii} is the distance between the i th interferer and its intended receiver. By doing this, we are actually inhibiting the interferers depending on their interference power, as received on the subject receiver, because the interferer's transmitted power is directly proportional to its own Tx-Rx separation under the proposed PPC. Through simulations and detailed analysis, we have demonstrated that the proposed algorithm significantly outperforms the well-known CSMA and network-wide fixed guard zone scheduling schemes [5].

The remainder of this article is organized as follows. Section 2 describes the assumptions and the network model used in this paper. Section 3 first explains the proposed scheduling scheme and then derivation of Ω^* in terms of the network parameters for the given system model. Afterwards, Section 4 compares the proposed scheme's results with the three major benchmarks, namely random aloha, the fixed-sized guard zone scheme, and the CSMA scheme. At the end, the work is concluded in Section 5.

2. The network model

We are generating a two-dimensional (2D) network of inhomogeneously distributed transmitters using [29]. First, we generate a homogeneous distribution of " N_i " transmitters according to the HPPP with intensity Λ_i ($nodes/m^2$). In this HPPP distribution, a node is defined to be a neighbor of another node if the distance between them is less than or equal to c . Now, to generate the inhomogeneous distribution, we apply a thinning algorithm as follows: each node in the initial homogeneous distribution is marked for thinning if it has fewer than k neighbors. After classifying the whole initial distribution, all the marked nodes are removed from the distribution to form a nonhomogeneous distribution of " N_o " transmitters with node density of Λ_o ($nodes/m^2$). To put it another way, a node is thinned if its k th nearest neighbor is at a distance greater than c . We are marking the nodes for thinning and then removing the marked nodes after completion of the classification for the whole distribution. Thus, the thinning process is independent of the sequence in which the nodes are processed by the thinning algorithm. An example of the thinning process is illustrated in Figure 2, where instead of Euclidean distance an approximate wrap-around distance is considered while counting the neighbors to mitigate the boundary effect which also affects the connectivity in ad-hoc networks [30]. After thinning, each surviving transmitter (Tx) has its own intended receiver (Rx), uniformly distributed in a disc of radius d_{max} , centered at that Tx. Therefore, the probability density function of Tx-Rx separations in the network is $f(x) = \frac{2x}{d_{max}^2}$.

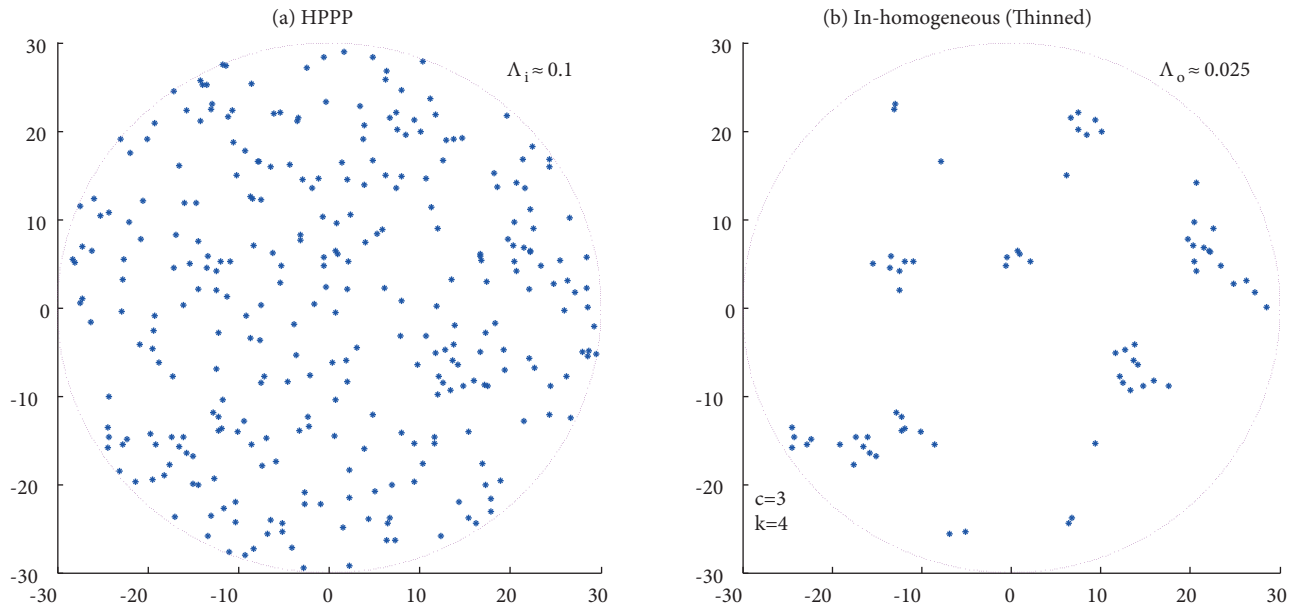


Figure 2. Nodes' distribution according to a homogeneous Poisson point process (left) and according to the inhomogeneous distribution (right) after implementing the explained thinning process on the initial homogeneous distribution. The illustration only shows a single realization of the homogeneous and thinned nodes and makes it easy to understand how the inhomogeneous distribution has been achieved.

In this paper, only single-hop transmissions are considered, where all the nodes have an omnidirectional antenna. Moreover, only matched filter receivers are considered with the spreading capability (DS-CDMA). Furthermore, the transmission capacity is defined as the maximum density of Tx-Rx pairs that can communicate successfully under some probability of outage (ν), whereas the transport capacity is defined as the sum of the lengths of all the successful communication links under some probability of outage (ν). We have utilized the distributed Pairwise Power Control (PPC) scheme [31] in our study. Under the PPC scheme, each transmitter chooses its transmission power to ensure that the received signal strength at the intended receiver remains constant, i.e. ρ . Therefore, the transmitter with Tx-Rx separation of d_{ii} will transmit $\rho(d_{ii})^\alpha$ under the PPC in a simple path-loss propagation model where α is the path-loss exponent.

The routing protocol determines which specific node requires single-hop communication; nonetheless, the accessibility to that particular node as well as the subsequent transmission is regulated by the channel access scheme. For this reason, an effective channel access scheme is undoubtedly inevitable and performs its own imperative work to delineate the network's transmission capacity. Furthermore, in order to perform a fair comparison of the two different access schemes, the contending schemes must be based on an identical routing scheme that could possibly be neglected during the comparison. In this study, a simple path-loss model has been considered for signal propagation while neglecting routing, energy efficiency, and end-to-end delays. The proposed scheme schedules the initially contending transmitters solely based on the guard zone criteria and any new Tx-Rx pair will be scheduled if and only if both the transmitter and the receiver are not violating the defined scheduling criteria for the already scheduled Tx-Rx pairs.

3. The proposed scheme and optimal multiplier's derivation

As explained in Section 1.1, the wise option is to incorporate an adaptive exclusion zone of radius $D = \Omega d_t$ to inhibit the interferer with Tx-Rx separation of d_t , where Ω is the network-wide fixed exclusion zone size multiplier or simply the exclusion zone multiplier.

Suppose a typical receiver (Rx_o) is positioned at the origin and it is receiving ρ from its own transmitter. Now, if (Rx_o) is guarded by an exclusion zone (EZ) of radius $D = \Omega d_{ii}$ to inhibit Tx_i , then each interferer will be suppressed depending on its own Tx-Rx separation (d_{ii}) and its distance (d_{io}) from the origin (Rx_o). Therefore, the probability that Rx_o will experience an outage will be P_{out}^{EZ} , as in Eq. (1), where G_s is the spreading gain, n is the narrow band channel noise and therefore Mn is the total noise in the wide band d_{ii} is the Tx-Rx separation of the i th Tx-Rx pair, d_{io} is the distance between the i th Tx (Tx_i) and Rx_o (i.e. the origin), and γ^* is the minimum SINR threshold for a successful communication link between two nodes:

$$P_{out}^{EZ} = P \left[\frac{\rho}{G_s n + \sum_{i \in (d_{io} > \Omega d_{ii})} \rho \left(\frac{d_{ii}}{d_{io}} \right)^\alpha} < \frac{\gamma^*}{G_s} \right]. \quad (1)$$

To derive an optimal exclusion zone multiplier parameter (Ω^*), we have to satisfy two constraints: the outage constraint and the spatial constraint. As per the first constraint, the probability of experiencing an outage at any typical receiver should not exceed some constant v . Therefore, we can formulate this constraint as in Eq. (2), which can also be written as Eq. (3). Here, $\delta = \frac{1}{\gamma^*} - \frac{n}{\rho}$, and $Y = \sum_{i \in (d_{io} > \Omega d_{ii})} \left(\frac{d_{ii}}{d_{io}} \right)^\alpha$ is the normalized (by ρ) total interference at the origin, following exclusion zone implementation:

$$P \left[\frac{\rho}{G_s n + \sum_{i \in (d_{io} > \Omega d_{ii})} \rho \left(\frac{d_{ii}}{d_{io}} \right)^\alpha} < \frac{\gamma^*}{G_s} \right] \leq v, \quad (2)$$

$$P[Y > G_s \delta] \leq v. \quad (3)$$

Using Campbell's theorem [31], for $\alpha > 2$, we can find the mean the μ_y with Eq. (4) and variance σ_y^2 with Eq. (5) of the normalized aggregate interference (Y) after employing the exclusion zone around Rx_o :

$$\mu_y = E[Y(\Lambda, \Omega)] = \frac{4\pi\Lambda}{d_{max}^2} \int_{x=0}^{d_{max}} \int_{r=\Omega x}^{\infty} r^{1-\alpha} x^{1+\alpha} dr dx = \frac{\pi\Omega^{(2-\alpha)} d_{max}^2 \Lambda}{\alpha - 2}, \quad (4)$$

$$\sigma_y^2 = E[Y^2(\Lambda, \Omega)] = \frac{4\pi\Lambda}{d_{max}^2} \int_{x=0}^{d_{max}} \int_{r=\Omega x}^{\infty} r^{1-2\alpha} x^{1+2\alpha} dr dx = \frac{\pi\Omega^{(2-2\alpha)} d_{max}^2 \Lambda}{2\alpha - 2}. \quad (5)$$

Now, in order to work out the optimal exclusion zone multiplier parameter (Ω^*), first we have to find the Y 's pdf. The closed form expression for this pdf was only found for a homogeneously distributed network with fixed Tx-Rx separations and zero exclusion zone [32]. However, for a network where transmitters are distributed according to the HPPP, the distribution of the aggregate interference from far-away nodes can be approximated by Gaussian distribution [33] after inhibiting the nearby interferers. Furthermore, as an outcome of the detailed simulations of the explained inhomogeneously distributed network under different network parameters, the distribution of the aggregate interference for a network of inhomogeneously distributed nodes is found to be equivalent to that of a network with nodes distributed according to the HPPP, as shown in Figure 3. Therefore,

we are assuming Gaussian distribution for Y , which is also validated through different simulations (shown in later sections). Thus, the outage constraint of Eq. (3) can be rewritten as in Eq. (6):

$$Q\left(\frac{G_s\delta - \mu_y}{\sigma_y}\right) \leq v. \quad (6)$$

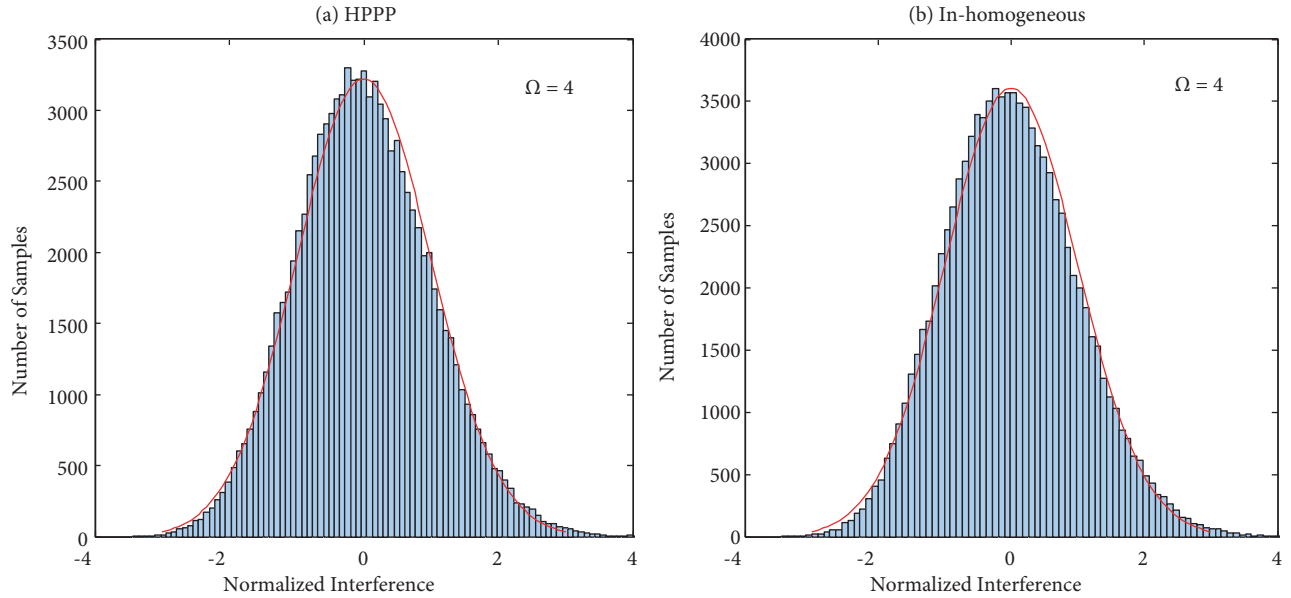


Figure 3. Comparison of the aggregate interference's distribution with Gaussian distribution for two different networks. The normalized aggregate interference's distribution inside a network of homogeneously distributed transmitters (left) and inside a network of inhomogeneously distributed transmitters (right).

The maximum density of transmitters Λ_{out} that can communicate simultaneously under the given outage constraint can be found by substituting Eqs. (4) and (5) in Eq. (6), which leads to Eq. (7):

$$\Lambda_{out} = \left[\frac{\theta_2}{2\theta_1\Omega} \left(\sqrt{1 + \frac{4\theta_1\delta\Omega^\alpha G_s}{\theta_2^2}} - 1 \right) \right]^2, (\alpha > 2), \quad (7)$$

where $\theta_1 = \frac{\pi d_{max}^2}{\alpha-2}$ and $\theta_2 = \sqrt{\frac{\pi}{2\alpha-2}} d_{max} Q^{-1}(v)$. However, this expression lacks the ability to solely illustrate the proposed scheme's benefits and limitations, because until now the exclusion zone has only been implemented around Rx_o . Therefore, the expression is not depicting the spatial constraint where each scheduled receiver will have an exclusion zone to inhibit the nearby interferers. In addition, according to this expression, there cannot be any communication link without implementing the exclusion zone ($\Omega = 0$). However, at low densities, the nodes are guaranteed to have spatial separation due to the intrinsic void probability of the PPP, which will help maintain some communication links [31].

Therefore, only one facet of the problem has been resolved by the outage constraint and now we have to introduce the spatial constraint, which will ensure our proposed exclusion zone around each scheduled receiver. Under the spatial constraint, only a percentage (p_t) of the initially contending transmitters will be permitted to transmit after inhibition of some of the transmitters with the execution of the proposed exclusion zone scheduling criteria, as evident from the flowchart in Figure 4. For a network with homogeneously distributed

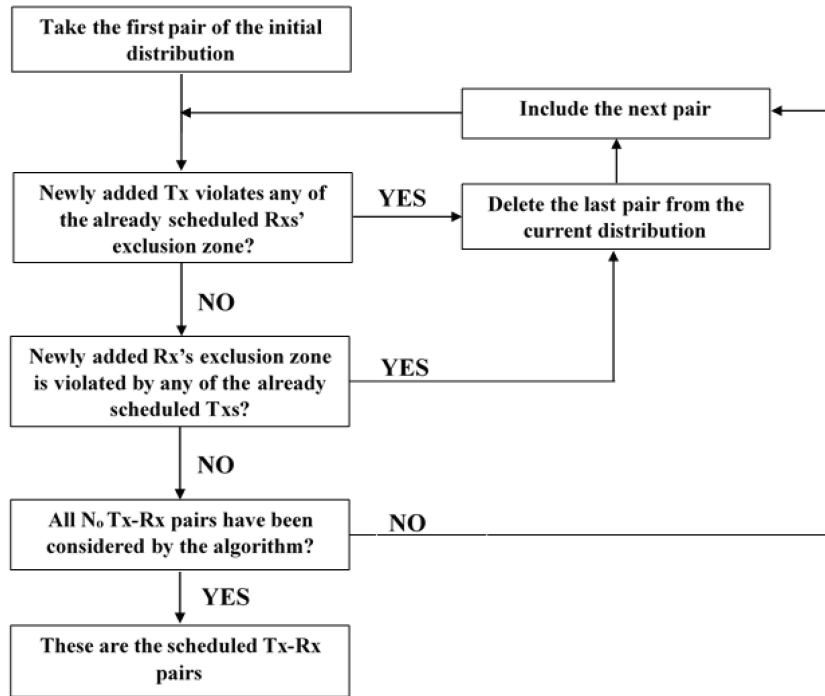


Figure 4. Flowchart for implementation of the proposed scheduling scheme. It is also evident that each active receiver employs the proposed adaptive guard zones to inhibit the interfering transmitters. The scheme analyzes all of the initially contending nodes and gives a scheduled subset of nodes where each scheduled Tx and Rx fulfills the proposed scheduling criteria.

nodes, p_t can be found using the void probability of the underlying PPP with node density Λ_o as in [16]. Although our system model has varied from the PPP after thinning, we are applying the expression for the PPP’s void probability to approximate p_t . The validity of this approximation is also substantiated by the results in the subsequent sections. Moreover, as the proposed exclusion zone’s radius depends on the interferer’s Tx-Rx separation and is not fixed, we have used the expected value of the exclusion zone’s radius to calculate the void probability. Therefore, $p_t = e^{-\frac{\Lambda_o \pi \Omega^2 d_{max}^2}{2}}$, and consequently the intensity of the transmitters that can communicate simultaneously under this spatial constraint is $\Lambda_s = \Lambda_o \times p_t$.

From the outset, our goal was to infer the optimal value of the exclusion zone multiplier (Ω^*), which allows the maximum number/intensity of Tx-Rx pairs (Λ^*) to communicate concurrently. Thus, the nonlinear optimization problem given in Eq. (8) has to be solved:

$$\Lambda(\Omega) = \max_{\Omega, \Lambda_o} [\min(\Lambda_s, \Lambda_{out})]. \tag{8}$$

Detailed numerical analysis shows that the value of Ω that maximizes $\Lambda(\Omega)$ is the value that results in $p_t \approx \frac{1}{e}$ over all the values of Λ_o . Analysis was performed for various network parameters, and the results for two of them are shown in Figure 5 and Figure 6. Therefore, the maximum intensity of Tx-Rx pairs that can transmit simultaneously under the spatial constraints, i.e. after the proposed exclusion zone implementation, is $\Lambda_s = \frac{2}{e\pi\Omega^2 d_{max}^2}$. Eventually, after equating Λ_s and Λ_{out} , the derived optimal exclusion zone multiplier Ω^*

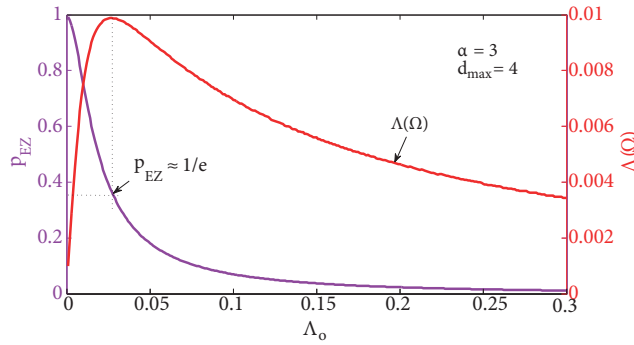


Figure 5. Plot of $\Lambda(\Omega)$ versus density of the initially contending nodes, where $\Lambda(\Omega)$ is maximized over all the values of Ω under different Λ_o , illustrating that the peak of $\Lambda(\Omega)$ occurs when $p_t \approx 1/e$, for $\alpha = 3$ and $d_{max} = 4m$.

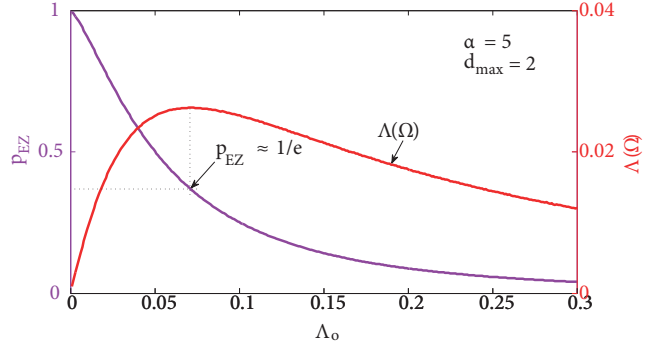


Figure 6. Plot of $\Lambda(\Omega)$ versus density of the initially contending nodes, where $\Lambda(\Omega)$ is maximized over all the values of Ω under different Λ_o , illustrating that the peak of $\Lambda(\Omega)$ occurs when $p_t \approx 1/e$, for $\alpha = 5$ and $d_{max} = 2m$.

and the corresponding (optimal) density Λ^* for DS-CDMA are found as in Eqs. (9) and (10):

$$\Omega^* = \left[\frac{\frac{2}{\alpha-2} + \sqrt{\frac{e}{\alpha-1}} Q^{-1}(v)}{G_s \delta e} \right]^{\frac{1}{\alpha}}, \quad (9)$$

$$\Lambda^* = \Lambda(\Omega^*) = \frac{2}{\pi d_{max}^2 e} \left[\frac{G_s \delta e}{\frac{2}{\alpha-2} + \sqrt{\frac{e}{\alpha-1}} Q^{-1}(v)} \right]^{\frac{2}{\alpha}}. \quad (10)$$

Naturally, the optimal value for the exclusion zone and the corresponding intensity depends on the network parameters and this relationship was examined by plotting the derived results against the different network parameters. As shown in Figure 7, the optimal exclusion zone multiplier decreases with a relaxation in the outage constraint because the relaxed outage allows more nodes to transmit simultaneously in the network, which results in a smaller exclusion zone. In addition, the plots also illustrate that a higher value of path-loss exponent supports smaller exclusion zones because of the high level of signal attenuation; however, at higher spreading gains, i.e. $G_s = 64$, the value of Ω^* increases with α , which could be due to $G_s \delta e > \frac{2}{\alpha-2} + \sqrt{\frac{e}{\alpha-1}} Q^{-1}(v)$. The analysis versus the spreading factor shows that Ω^* is inversely proportional to G_s . Furthermore, at a higher value of G_s , a carrier sensing scheme is not mandatory because the exclusion zone multiplier falls below unity.

Similarly, the effect of different network parameters on the optimal transmission capacity ($\Lambda^* = \Lambda(\Omega^*)$) is shown in Figure 8. It shows that, irrespective of the G_s and α 's values, Λ^* is directly proportional to v because the relaxed outage constraint allows the nodes to be densely packed within the network. Moreover, for any given values of v and d_{max} , Λ^* increases with α for $G_s = 1$ while it decreases with α at $G_s = 64$, which possibly results in $G_s \delta e > \frac{2}{\alpha-2} + \sqrt{\frac{e}{\alpha-1}} Q^{-1}(v)$. It is also evident from Eq. (10) that the larger d_{max} resists the simultaneous transmission by a larger number of nodes and therefore deteriorates the transmission capacity.

The optimal exclusion zone multiplier Ω^* was also found for various network settings through simulations (without the Gaussian assumption for aggregate interference's distribution) for comparison with the results derived from Eq. (9) and are plotted in Figure 9 and Figure 10. While using the network parameters of the Table, the described network model was simulated and the results were averaged over thousands of realizations. The

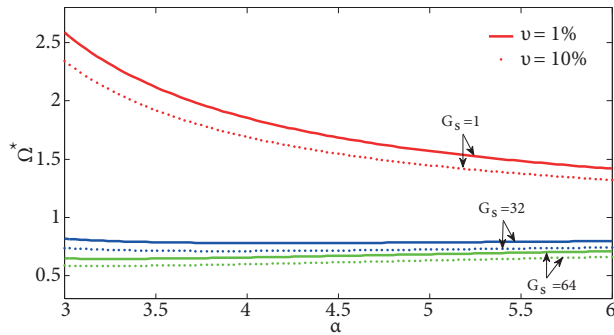


Figure 7. The optimal exclusion zone multiplier (Ω^*) vs. the path-loss exponent (α) for different values of v and G_s , showing that Ω^* decreases with path loss in a narrow-band system but becomes almost insensitive to α at higher values of G_s .

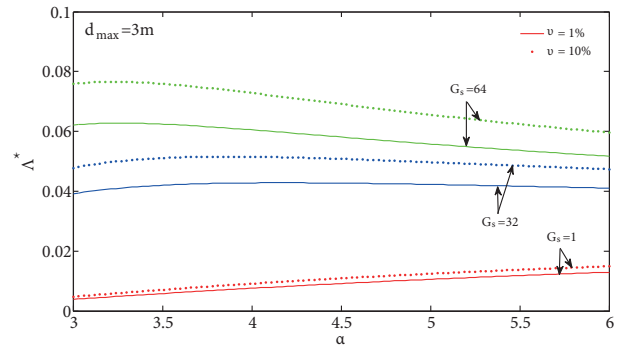


Figure 8. The optimal transmission capacity (Λ^*) vs. the path-loss exponent (α) for different values of v and G_s , showing that the Λ^* linearly increases with path loss in a narrow-band system but becomes inversely proportional to α at higher values of α and G_s .

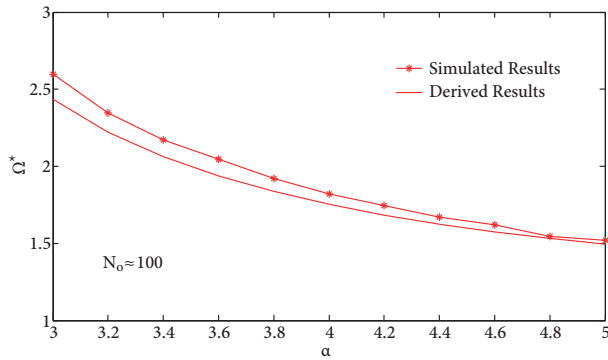


Figure 9. The derived (with the Gaussian and void probability's assumption) and the simulated (without any assumption) Ω^* plotted against α . This plot shows the inverse relationship between the optimal exclusion zone multiplier and the network's path-loss exponent, and it validates our assumptions, as well.

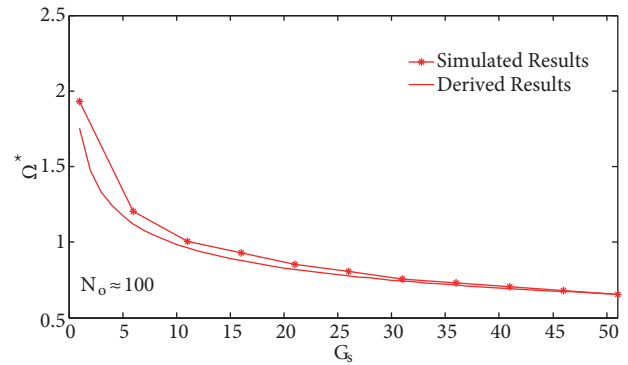


Figure 10. The derived (with the Gaussian and void probability's assumption) and the simulated (without any assumption) Ω^* plotted against G_s . This plot shows the inverse relationship between the optimal exclusion zone multiplier and the network's spreading gain, and it substantiates our assumptions as well.

Table. Network parameters, unless otherwise specified.

Symbol	Description	Value
R	Network radius	30 m
n	Receiver noise	0.001
v	Probability of outage	0.05
α	Path-loss exponent	4
γ^*	Minimum required SINR	10 dB
d_{max}	Maximum allowed Tx-Rx separation	4 m
c	Maximum allowed distance between two neighboring transmitters	5 m
k	Minimum number of neighbors to survive thinning process	9
G_s	Spreading gain	1

results not only validated our derivation, but also validated the void probability and the Gaussian assumption regarding the interference's distribution because the derived results (with assumptions) are closely followed by the simulation results (without assumptions).

4. Proposed scheme's performance analysis and discussion

A detailed analysis of the proposed scheme's performance was also carried out while making a comparison with well-known existing schemes. The comparison was performed through extensive simulations of all the schemes where the considered benchmarks include random aloha, the system-wide fixed exclusion zone scheme, and the widely used CSMA scheme. The Monte Carlo simulations were run and plots were plotted in MATLAB R2012a. For comparison, different algorithms were applied to the same distribution of contending nodes for a single network realization and averaged over thousands of network realizations to get realistic and reliable results/plots.

4.1. Adaptive exclusion zone versus random aloha (i.e. $\Omega = 0$)

The aloha scheme is tantamount to applying the power control scheme on the inhomogeneously distributed contending nodes without any scheduling. The proposed scheme provided a substantial increase in the transmission capacity that is denoted by $G_{ALOHA} = \frac{\Lambda^*}{\Lambda_{ALOHA}}$, where Λ_{ALOHA} is the transmission capacity under the random aloha scheme.

Figure 11 shows that the suggested scheme gives an increase of approximately 100-fold in the transmission capacity at moderate path-loss exponent and higher node density in a narrow-band system. It is also evident that the proposed scheme's benefits are much more significant for a network with larger d_{max} because the random aloha's performance deteriorates with increasing Tx-Rx separation. Moreover, G_{ALOHA} is inversely proportional to the path-loss exponent because higher path loss favors random aloha by providing higher attenuation and thus mitigating the need for an efficient scheduling scheme.

These outcomes are somewhat intuitive due to the known superiority of the scheduling over the random aloha scheme; even so, the subsequent sections illustrate the real strength of the proposed scheme, where it is compared to the well-known distributed scheduling schemes for ad hoc networks.

4.2. Adaptive exclusion zone versus fix-sized exclusion zone

An optimal but fixed-sized exclusion zone was proposed in [16] for a homogeneously distributed wireless network with fixed Tx-Rx separation and then utilized in [5] for a wireless network with variable Tx-Rx separation. This algorithm showed substantial improvement in the transmission as well as in the transport capacity when compared to the other well-known scheduling schemes [5]. For comparison, we have simulated this scheme along with our proposed scheme for the inhomogeneously distributed network of Section 2. The proposed scheme provided a significant gain in the transmission and transport capacity when compared to the fixed-sized exclusion zone. This gain in capacity is denoted by $G_{Fixed} = \frac{\Lambda^*}{\Lambda_{Fixed}}$, where Λ_{Fixed} is the capacity under the fixed-sized exclusion zone scheme.

In Figure 12, the proposed scheme's gain in transmission capacity $G_{Transmission}$ and gain in transport capacity $G_{Transport}$, as compared to the fixed-sized guard zone scheme, are plotted against the number of initially contending nodes (N_o) for two different values of d_{max} . The plots clearly signify the strength of the proposed scheme by showing that both $G_{Transmission}$ and $G_{Transport}$ are directly proportional to d_{max} where increasing d_{max} provides a significant gain to the proposed scheme. As the proposed scheme is good at enhancing the transmission capacity by efficiently making room for the nodes with small Tx-Rx separations, the proposed scheme's transmission gain outperforms the transport gain. Moreover, as compared to the fixed exclusion zone, the proposed scheme provides more than 31% gain in the transmission capacity in a narrow-band system with a larger d_{max} at a moderate value of α (i.e. $\alpha = 4$).

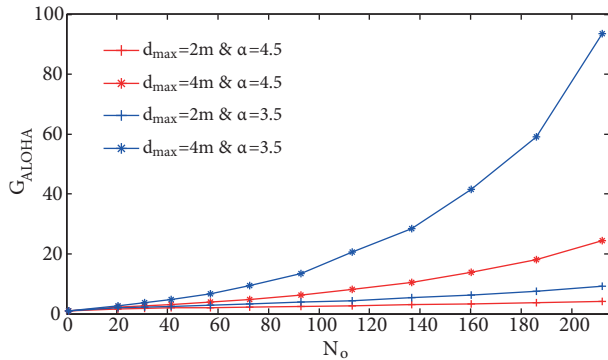


Figure 11. Gain in transmission capacity G_{ALOHA} plotted against the number of nodes contending for channel N_o for different values of d_{max} and α .

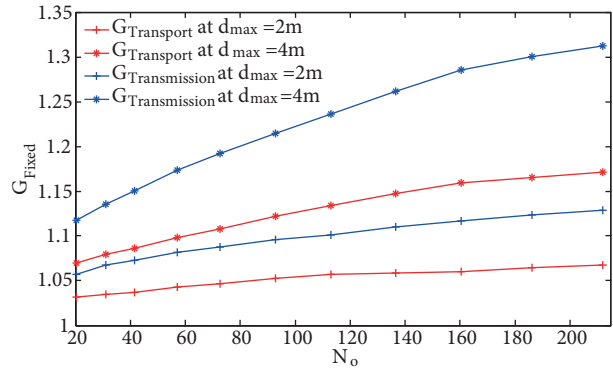


Figure 12. The gains achieved by the proposed scheme in transmission capacity ($G_{Transmission}$) and transport capacity ($G_{Transport}$) as compared to the fixed-sized guard zone scheme, plotted against the number of initially contending nodes (N_o) for different values of d_{max} .

4.3. Proposed scheme versus CSMA

The CSMA scheme [20] is one of the most well-known and widely used distributed scheduling schemes. The proposed scheme's performance is also compared to the CSMA scheme to emphasize its strength and benefits by simulating the CSMA scheme for the explained nonhomogeneously distributed network. The proposed scheme provided a substantial gain in transmission and transport capacity when compared to the CSMA. This gain in the capacity is denoted by $G_{CSMA} = \frac{\Lambda^*}{\Lambda_{CSMA}}$, where Λ_{CSMA} is the capacity under the CSMA scheme.

Figure 13 shows the effect of different network parameters on G_{CSMA} . G_{CSMA} witnesses a constant rate of increase with α in a narrow-band ($G_s = 1$) system for $\alpha \leq 7$. On the other hand, the rate of increase decreases with α in a system with higher spreading gain. The plot also shows that the narrow-band system outperforms the spread-spectrum for higher values of path loss (i.e. $\alpha \geq 6.5$), because at such a high, otherwise unrealistic path loss [34, 35] the terms $[-\frac{2}{\alpha-2} + \sqrt{\frac{e}{\alpha-1}Q^{-1}(v)}]$ and $(\frac{2}{\alpha})$ are dominant in Eq. (10). However, at moderate values of the path-loss exponent (α), the proposed scheme provides about 60% gain in the transmission capacity.

In Figure 14, the proposed scheme's gain in transmission capacity $G_{Transmission}$ and gain in transport capacity $G_{Transport}$ are plotted against the number of initially contending nodes (N_o) for two different values of d_{max} . The plots show that both $G_{Transmission}$ and $G_{Transport}$ are directly proportional to d_{max} and doubling the d_{max} provides a significant edge to the proposed scheme. In addition, the proposed scheme's transmission gain outperforms the transport gain because it is better at scheduling the nodes with smaller Tx-Rx separation. Although $G_{Transport}$ is slightly lower than $G_{Transmission}$, it holds a considerable value of ≈ 1.45 for a narrow-band network with higher node density and larger d_{max} .

5. Conclusion

This article has verified that the nearest interferer is not guaranteed to be the dominant one, and has also proposed an adaptive scheduling strategy that is in some way foreseeing each interferer's transmitted power to make a decision pertaining to its inhibition. In this article, we have also derived an optimal exclusion-zone multiplier as a function of the network's variables.

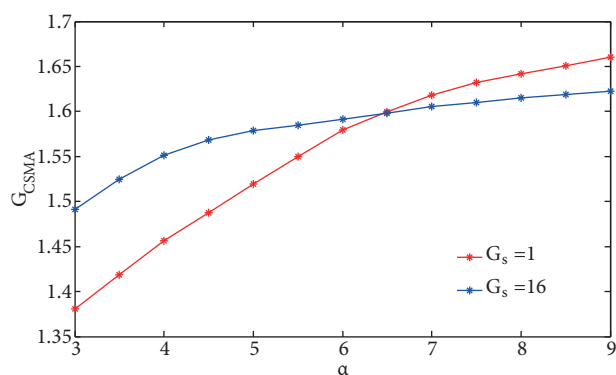


Figure 13. The gain in transmission capacity G_{CSMA} plotted against the path-loss exponent α , both for the narrow-band ($G_s = 1$) and the spread-spectrum ($G_s = 16$) networks.

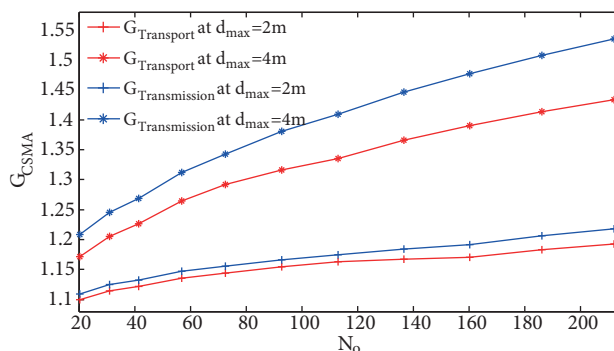


Figure 14. The gains achieved by the proposed scheme in the transmission capacity ($G_{Transmission}$) and transport capacity ($G_{Transport}$), as compared to the CSMA scheme, plotted against the number of initially contending nodes (N_o) for different values of d_{max} .

The evaluation of the proposed strategy has also manifested its benefits over other benchmarks such as random aloha, the fixed-sized guard zone scheme, and the CSMA scheme. The proposed algorithm not only outperformed random aloha but also surpassed the other schemes by a significant margin. Moreover, under the proposed scheme, the exclusion-zone multiplier may have a value less than unity, which eventually eradicates the need for a carrier sensing mechanism. Furthermore, the suggested algorithm is as convenient to employ as the other benchmarks.

References

- [1] Qiu T, Chen N, Li K, Qiao D, Fu Z. Heterogeneous ad hoc networks: architectures, advances and challenges. Ad Hoc Networks 2017; 55: 143-152. doi: 10.1016/j.adhoc.2016.11.001
- [2] Hwang I, Song B, Soliman S. A holistic view on hyper-dense heterogeneous and small cell networks. IEEE Communications Magazine 2013; 51 (6): 20-27. doi: 10.1109/MCOM.2013.6525591
- [3] Asadi A, Wang Q, Mancuso V. A survey on device-to-device communication in cellular networks. IEEE Communications Surveys Tutorials 2014; 16 (4): 1801-1819. doi: 10.1109/COMST.2014.2319555
- [4] Kim J, Lee J, Kim J, Yun J. M2M service platforms: survey, issues, and enabling technologies. IEEE Communications Surveys Tutorials 2014; 16 (1): 61-76. doi: 10.1109/SURV.2013.100713.00203
- [5] Hasan A, Ali A. Guard zone-based scheduling in ad hoc networks. Computer Communications 2015; 56: 89-97. doi: 10.1016/j.comcom.2014.11.004
- [6] Ajmal S, Jabeen S, Rasheed A, Hasan A. An intelligent hybrid spread spectrum MAC for interference management in mobile ad hoc networks. Computer Communications 2015; 72: 116-129. doi: 10.1016/j.comcom.2015.04.006
- [7] Mao Y, Yan F, Shen L. Multi-round elimination contention-based multi-channel MAC scheme for vehicular ad hoc networks. IET Communications 2017; 11 (3): 421-427. doi: 10.1049/iet-com.2016.0774
- [8] Li X, Zhang Y, Zhao S, Shen Y, Jiang X. Exact secrecy throughput capacity study in mobile ad hoc networks. Ad Hoc Networks 2018; 72: 105-114. doi: 10.1016/j.adhoc.2018.01.012
- [9] Pala Z, İnanç N. The impact of disabling suspicious node communications on network lifetime in wireless ad hoc sensor networks. Turkish Journal of Electrical Engineering & Computer Sciences 2016; 24 (5): 4429-4444. doi: 10.3906/elk-1411-198

- [10] Sivakumar T, Manoharan R. ERP: An efficient reactive routing protocol for dense vehicular ad hoc networks. *Turkish Journal of Electrical Engineering & Computer Sciences* 2017; 25 (3): 1762-1772. doi: 10.3906/elk-1507-147
- [11] Su H, Moh S. A robust deafness-free MAC protocol for directional antennas in ad hoc networks. *Wireless Personal Communications* 2017; 96 (1): 1111-1129. doi: 10.1007/s11277-017-4227-y
- [12] Pourgolzari V, Ghorashi S. A CDMA based MAC protocol for ad hoc networks with directional antennas. In: *Proceedings of International Symposium on Computer Networks and Distributed Systems*; Tehran, Iran; 2011. pp. 73-77.
- [13] Zhang J, Dziong Z, Gagnon F, Kadoch M. Multiuser detection based MAC design for ad hoc networks. *IEEE Transactions on Wireless Communications* 2009; 8 (4): 1836-1846. doi: 10.1109/T-WC.2008.071449
- [14] Ganti RK, Haenggi M. Interference and outage in clustered wireless ad hoc networks. *IEEE Transactions on Information Theory* 2009; 55 (9): 4067-4086. doi: 10.1109/TIT.2009.2025543
- [15] Torrieri D, Valenti MC. Exclusion and guard zones in DS-CDMA ad hoc networks. *IEEE Transactions on Communications* 2013; 61 (6): 2468-2476. doi: 10.1109/TCOMM.2013.041113.120714
- [16] Hasan A, Andrews J. The guard zone in wireless ad hoc networks. *IEEE Transaction on Wireless Communications* 2007; 6 (3): 897-906. doi: 10.1109/TWC.2007.04793
- [17] Schilcher U, Brandner G, Bettstetter C. Quantifying inhomogeneity of spatial point patterns. *Computer Networks* 2017; 115: 65-81. doi: 10.1016/j.comnet.2016.12.018
- [18] Mukherjee S, Avidor D. Outage probabilities in Poisson and clumped Poisson-distributed hybrid ad-hoc networks. In: *Second Annual IEEE Communications Society Conference on Sensor and Ad Hoc Communications and Networks*; Santa Clara, CA, USA; 2005. pp. 563-574.
- [19] Alfano G, Garetto M, Leonardi E. Capacity scaling of wireless networks with inhomogeneous node density: Lower bounds. In: *28th IEEE Conference on Computer Communications*; Rio de Janeiro, Brazil; 2009. pp. 1890-1898.
- [20] IEEE. Standard for Information Technology - Local and Metropolitan Area Networks - Specific Requirements - Part 11: Wireless LAN Medium Access Control (MAC) and Physical Layer (PHY) Specifications, Amendment 8: IEEE 802.11 Wireless Network Management. *IEEE Std 802.11v-2011*. New York, NY, USA: IEEE, 2011. doi: 10.1109/IEEESTD.2011.5716530
- [21] Sial N, Ahmed J. A novel and realistic hybrid downlink-uplink coupled/decoupled access scheme for 5G HetNets. *Turkish Journal of Electrical Engineering & Computer Sciences* 2017; 25 (6): 4457-4473. doi: 10.3906/elk-1612-167
- [22] Tian J, Zhang H, Wu D, Yuan D. QoS-constrained medium access probability optimization in wireless interference-limited networks. *IEEE Transactions on Communications* 2018; 66 (3): 1064-1077. doi: 10.1109/TCOMM.2017.2775239
- [23] Baccelli F, Blaszczyszyn B, Muhlethaler P. An Aloha protocol for multihop mobile wireless networks. *IEEE Transactions on Information Theory* 2006; 52 (2): 421-436. doi: 10.1109/TIT.2005.862098
- [24] Yang X, Veciana G. Inducing multiscale clustering using multistage MAC contention in CDMA ad hoc networks. *IEEE/ACM Transactions on Networking* 2007; 15 (6): 1387-1400. doi: 10.1109/TNET.2007.902690
- [25] Muqattash A, Krunz M. CDMA-based MAC protocol for wireless ad hoc networks. In: *Proceedings of the 4th ACM International Symposium on Mobile Ad Hoc Networking & Computing*; Annapolis, MD, USA; 2003. pp. 153-164.
- [26] Gupta P, Kumar PR. The capacity of wireless networks. *IEEE Transactions on Information Theory* 2000; 46 (2): 388-404. doi: 10.1109/18.825799
- [27] Afshang M, Saha C, Dhillon HS. Nearest-neighbor and contact distance distributions for Thomas cluster process. *IEEE Wireless Communications Letters* 2017; 6 (1): 130-133. doi: 10.1109/LWC.2016.2641935
- [28] Afshang M, Saha C, Dhillon HS. Nearest-neighbor and contact distance distributions for Matérn cluster process. *IEEE Communications Letters* 2017; 21 (12): 2686-2689. doi: 10.1109/LCOMM.2017.2747510

- [29] Bettstetter C, Gyarmati M, Schilcher U. An inhomogeneous spatial node distribution and its stochastic properties. In: Proceedings of the 10th ACM Symposium on Modeling, Analysis, and Simulation of Wireless and Mobile Systems; Chania, Greece; 2007. pp. 400-404.
- [30] Santi P, Blough DM. The critical transmitting range for connectivity in sparse wireless ad hoc networks. IEEE Transactions on Mobile Computing 2003; 2 (1): 25-39. doi: 10.1109/TMC.2003.1195149
- [31] Weber SP, Yang X, Andrews J, Veciana G. Transmission capacity of wireless ad hoc networks with outage constraints. IEEE Transactions on Information Theory 2005; 51 (12): 4091-4102. doi: 10.1109/TIT.2005.858939
- [32] Sousa ES, Silvester J. Optimum transmission ranges in a direct-sequence spread-spectrum multihop packet radio network. IEEE Journal on Selected Areas in Communications 1990; 8 (4): 762-771. doi:10.1109/49.56383
- [33] Aljuaid M, Yanikomeroglu H. Investigating the Gaussian convergence of the distribution of the aggregate interference power in large wireless networks. IEEE Transactions on Vehicular Technology 2010; 59 (9): 4418-4424. doi: 10.1109/TVT.2010.2067452
- [34] Rappaport TS. Wireless Communications: Principles and Practice. 2nd ed. Upper Saddle River, NJ, USA: Prentice Hall, 2002.
- [35] Miranda J, Abrishambaf R, Gomes T, Gonçalves P, Cabral J et al. Path loss exponent analysis in wireless sensor networks: Experimental evaluation. In: 11th IEEE International Conference on Industrial Informatics; Bochum, Germany; 2013. pp. 54-58.